Non-linear Dependence of L_B on L_{FIR} and M_{H_2} among Spiral Galaxies and Effects of Tidal Interaction

J. Perea, A. del Olmo, L. Verdes-Montenegro

Instituto de Astrofísica de Andalucía, CSIC, Apdo. 3004, 18080 Granada, Spain.
(jaime@iaa.es, chony@iaa.es, lourdes@iaa.es)

and

M. S. Yun

National Radio Astronomy Observatory[1]*, P.O. Box 0, Soccoro, NM 87801 (myun@nrao.edu)*

ABSTRACT

Through the study of a carefully selected sample of isolated spiral galaxies, we have established that two important global physical quantities for tracing star forming activities, L_{FIR} and M_{H_2}, have non-linear dependence on another commonly cited global quantity L_B. Furthermore we show that simple power law relations can effectively describe these non-linear relations for spiral galaxies spanning four orders of magnitude in FIR and M_{H_2} and nearly three orders of magnitude in L_B. While the existence of non-linear dependence of M_{H_2} (assuming a constant CO-to-H_2 conversion) and L_{FIR} on optical luminosity (L_B) has been previously noted in the literature, an improper normalization of simple scaling by L_B has been commonly used in many previous studies to claim enhanced molecular gas content and induced activities among tidally interacting and other types of galaxies. We remove these non-linear effects using the template relations derived from the isolated galaxy sample and conclude that *strongly interacting galaxies do not have enhanced molecular gas content*, contrary to previous claims. With these non-linear relations among L_B, L_{FIR} and M_{H_2} properly taken into account, we confirm again that the FIR emission and the star formation efficiency (L_{FIR}/M_{H_2}) are indeed enhanced by tidal interactions. Virgo galaxies show the same level of M_{H_2} and L_{FIR} as isolated galaxies. We do not find any evidence for enhanced star forming activity among barred galaxies.

Subject headings: galaxies: fundamental parameters — galaxies: interactions — galaxies: ISM — infrared: galaxies — radio lines: galaxies

[1]The National Radio Astronomy Observatory is a facility of the National Science Foundation operated under cooperative agreement by Associated Universities, Inc.

1. Introduction

The molecular gas (H_2) and far-infrared (FIR) contents are important quantities in analyzing the star formation activity in galaxies. They have been analyzed in the literature for different galaxy samples (Young & Scoville 1991 and references therein, Sofue et al. 1993, Braine & Combes 1993, Young et al. 1996, Solomon et al. 1997) although largely among the IR luminous galaxies. These two quantities correlate linearly assuming a constant CO-to-H_2 conversion factor, and massive star formation within molecular clouds is sufficient to explain the observed trend in most cases. On the other hand, several authors have noted that these quantities do *not* correlate linearly with the total blue luminosity (L_B) in the sense that M_{H_2}/L_B and L_{FIR}/L_B increase with increasing L_B (Young 1987, Young et al. 1989, Sage & Solomon 1989). Nevertheless, a simple normalization using L_B has been commonly used to claim enhanced activities among different groups of galaxies (e.g., Braine & Combes 1993, Combes et al. 1994, Devereux & Hameed 1997) while what they have actually shown is this residual dependence on the luminosity. In this paper, we first examine the nature of non-linearity involving L_B, and then re-examine the previous claims of enhanced molecular gas content and star forming activity based on the normalization by L_B. We show here that the enhanced molecular gas content among bright interacting galaxies reported in the literature is entirely due to the non-linearity effect, but the excess in the FIR emission is real and is largely due to real enhancement induced by environmental effects.

We have compiled from the literature an extensive comparison sample of 207 galaxies in varying interaction classes and environment (isolated, weakly perturbed, strongly perturbed, Virgo cluster), representing a wide range of optical luminosity ($10^{8.6}\ L_\odot < L_B < 10^{11.4}\ L_\odot$) and for which FIR, CO, and optical luminosity (as measured by the blue luminosities L_B) are available. The FIR luminosity is obtained as $log(L_{FIR}/L_\odot) = log(FIR) + 2log(D) + 19.495$ where D is distance in Mpc and $FIR = 1.26 \times 10^{-14} \times (2.58 I_{60} + I_{100})$ W m^{-2} (Helou et al. 1988). The 60 μm and 100 μm fluxes are obtained from the NED[2] database. The molecular hydrogen mass is derived as $M_{H_2} = 4.82\ \alpha I_{CO} d_B^2\ M_\odot$, assuming a constant CO-to-H_2 conversion factor of $\alpha = N_{H_2}/I_{CO} = 3 \times 10^{20}$ cm^{-2} (K km s^{-1})$^{-1}$, where I_{CO} is the velocity integrated CO intensity in K km s^{-1} and d_B is the half-power beam diameter in pc at the source distance (Sanders et al. 1991). The use of a constant conversion factor is discussed further in § 2. Because many nearby galaxies typically subtend several arcmin in size and are much larger than the beam of the telescopes used, the comparison data consist mostly of the CO surveys using at least partial mapping. The optical luminosity is derived from the B_T^0 magnitude from the RC3 catalogue, corrected for galactic absorption (using the extinction value given by Burstein & Heiles 1984, with the reddening law from Savage & Mathis 1979) and internal extinction (de Vaucouleurs et al. 1991 RC3) using the redshift given in NED. We adopted a value for the Hubble constant of $H_0 = 75$ km s^{-1} Mpc^{-1}.

2. Relationship among L_B, L_{FIR} and M_{H_2} for Isolated Galaxies

In order to first understand the intrinsic non-linear nature of L_B with respect to FIR luminosity and molecular gas content, we have assembled from the literature a reference sample of isolated galaxies representing a wide range of luminosity that extends from $L_B = 10^{8.6}$ to $10^{10.9}\ L_\odot$. Our isolated galaxy sample consists of 68 objects from the distance limited survey of the Nearby Galaxies Catalog (Tully 1988) by Sage (1993) and the class 0 objects of the IRAS selected sample by

[2] The NASA/IPAC Extragalactic Database (NED) is operated by the Jet Propulsion Laboratory, California Institute of Technology, under contract with the National Aeronautics and Space Administration.

Solomon & Sage (1988). For six galaxies only upper limits are available on the CO luminosity. Morphological types range from Sa to Sd galaxies, each distributed along the entire luminosity range, and the types around Sc are the most abundant. This sample lacks completeness because the galaxies studied in the literature are frequently biased towards infrared luminous galaxies. On the other hand, our isolated galaxy sample is sufficient for this comparison study in the sense that the range of optical luminosity present in other comparison samples are basically included.

In Fig. 1a, we plot L_B against M_{H_2} for this sample. The data can be well described by a simple power law relation

$$log L_B = (0.57 \pm 0.03)\, log M_{H_2} + (4.9 \pm 0.6) \quad (1)$$

The coefficients are determined by a linear regression taking into account the upper limits using the Astronomy Survival Analysis package (ASURV[3]). We do not find any dependence on the morphological types. Sage & Solomon (1989) report a slope of 0.53 ± 0.07 for a sample of isolated and weakly perturbed galaxies, and Young et al. (1989) find a slope of 0.72 ± 0.03 for a sample of 124 galaxies with CO data. Removing the 5 nearby dwarf galaxies with lowest luminosities ($L_B < 7 \times 10^7$ $L_\odot$) that clearly separate from the overall tendency, we find a slope of 0.54 for the Young et al. sample – which is consistent with our result.

In Fig. 1b we plot L_{FIR} against M_{H_2}, whose ratio is a measure of the star formation efficiency (SFE) (see Young & Scoville 1991). This correlation has been widely considered in the literature and found to be nearly linear when a large range of luminosities are considered,

$$log L_{FIR} = (0.90 \pm 0.05)\, log M_{H_2} + (1.5 \pm 0.4) \quad (2)$$

with a similar dispersion as that of L_B-M_{H_2} relation.

These plots demonstrate that L_B increases more slowly compared with the molecular gas content (for a constant CO-to-H_2 conversion factor) and far-infrared luminosity, and more importantly, these non-linear dependencies are present even among these carefully selected isolated spirals. While the physical cause for the observed non-linear relations is uncertain, it is suggestive that the physical mechanism responsible for the FIR and CO (M_{H_2}) emission may be closely related, but they are distinct in nature from optical emission. For the ease of the subsequent discussions, we have parameterized the above empirical non-linear relations in terms of M_{H_2}, but we do not claim that M_{H_2} (or any of the three physical quantities compared here) is the fundamental driver.

If one postulates that the root of the non-linear relations shown in Eqs. 1 & 2 lies in the FIR and CO emission, then an obvious possible cause is the metallicity dependence on the luminosity. In fact, a positive correlation between metallicity and absolute magnitude has been obtained by Roberts & Haynes (1994) for a large sample of spiral galaxies, and Arimoto et al. (1996) have proposed an empirical dependence between CO–to–H_2 conversion and absolute magnitude based on their observational data and the CO emission model of Sakamoto (1996). Indeed there are clear indications that the CO intensity may not be a good tracer of the molecular content among metal–poor galaxies (Cohen et al. 1988, Rubio et al. 1991). Also, the non-linear dependence in Eq. 1 is nearly reproduced by the metallicity dependence derived by Roberts & Haynes if the CO emission is assumed to depend linearly on the metallicity. However, there are observational and theoretical reasons to believe that such a metallicity dependence cannot work. For example, the observational evidence for metallicity dependence offered by Arimoto et al. becomes marginal if the low spatial resolu-

[3] Astronomy Survival Analysis (ASURV) Rev 1.2 package is a generalized statistical analysis package which implements the methods presented by Feigelson & Nelson (1985) and Isobe et al. (1986) and are described in detail in Isobe & Feigelson (1990) and La Valley et al. (1992)

tion data on M51 and LMC are removed. Also, full chemical and radiative transfer modeling of CO emission by Wolfire, Hollenbach, & Tielens (1993) and Maloney & Wolfire (1997) suggests that CO emission is a robust tracer of M_{H_2} against metallicity variation – no metallicity dependence is expected until the metal abundance becomes low enough to make the CO transition optically thin.

Alternatively if the non-linear relations derived above are rooted in L_B, then optical extinction and scattering model may offer an explanation. A naive expectation is that larger extinction in more massive galaxies with larger dust column density would result in a slower increase in L_B with size (e.g., Young et al. 1989). Buat & Xu (1996) also find a good correlation between the optical depth in B and the ratio of FIR to blue luminosity. Therefore, it is natural to suspect that the root of the observed non-linearity may lie with L_B rather than with L_{FIR} or M_{H_2}.

In a simple geometrical extinction model in which optically thick tracers such as blue light represent surface area and optically thin tracers such as FIR and integrated CO intensity represent volume elements, a non-linear dependence is naturally expected between these two classes of tracers – i.e., $L_B \propto [M_{H_2}]^{2/3}$ for a spherical uniform cloud. In reality, the structure of the ISM is more complex and clumpy or filamentary, and the effective optical depth is significantly reduced compared with a uniform screen model by extinction geometry and efficient scattering (Witt et al. 1992, 1996). Nevertheless, it is remarkable that the non-linear relation between L_B and M_{H_2} is observed with nearly the same power law dependence as predicted by this simple model, and one may infer that the basic assumptions of the model stated above must hold at the clump-interclump size scales. We note that the predicted exponent of 2/3 is independent of the cloud shape as long as the cloud structure remains self-similar at different size scales.

The extinction model also correctly predicts other optical depth dependent trends. For example, the exponent of the correlation between L_B and L_{FIR} is expected to be *steeper* than that of L_B–M_{H_2} because additional surface element provided by HI among the low luminosity galaxies is partly compensated in FIR by the dust emission associated with the HI gas. A formal fit for the L_B–L_{FIR} relation in our isolated galaxy sample gives

$$log L_B = (0.65 \pm 0.09)\, log L_{FIR} + (3.9 \pm 0.9) \quad (3)$$

and the slope of the correlation is indeed larger than that of L_B–M_{H_2} (0.57 ± 0.03). We predict that the optical luminosity at longer wavelengths (L_H or L_K) would produce a more linear relationship with M_{H_2} than L_B.

3. Re-evaluation of the Tidal and Environmental Effects

Regardless of their physical causes, two global physical quantities L_{FIR} and M_{H_2} show clearly non-linear dependence with respect to L_B among a large sample of isolated galaxies. The relations are well described by a simple power law spanning four orders of magnitude in L_{FIR} and M_{H_2} and nearly three orders of magnitude in L_B (see §2). Therefore, any comparison of L_{FIR} and M_{H_2} normalized simply by L_B produce a misleading result. This is particularly true for the studies of bright interacting galaxies found in the literature where the samples are often selected based on their high luminosity. Here we re-evaluate the impact of tidal and environmental effects on individual galaxies by examining their global properties using the empirical relations derived from our isolated galaxy sample as templates in order to discriminate the size–dependent effects from the environmentally induced effects. Deviations from the template power laws (Eqs. 1 & 2) are evaluated below for galaxies suffering different degrees of interactions. We also examine whether the presence of a bar correlates with any enhancement in the star formation efficiency. While each subsamples analyzed here represent different range of luminosity with different mean luminosity, almost the entire range of optical luminosity considered are represented in our isolated galaxy sample, and the use of these template relations are justified.

Both the FIR and CO data available in the literature are severely sensitivity limited, and a special care has to be made to incorporate the upper limits properly in the analysis. Standard statistical tests such as Kolmogorov–Smirnov (KS) or Mann–Whitney cannot be rigorously applied to these heavily censored data, and we instead use equivalent tests provided by ASURV. In particular to quantify the statistical probability of the compared samples representing the same distribution function, we use the logrank and Peto–Prentice generalized Wilcoxon test which are known to be the most robust against the censoring pattern.

3.1. Interacting and Cluster Galaxies

The entire sample studied here consists of 139 galaxies, divided into three subclasses: weakly perturbed (WP), strongly perturbed (SP), and Virgo Cluster (VC) galaxies. The WP sample has 43 galaxies including interaction class 1, 2 & 3 of Solomon & Sage (1988) and class 2 objects from the luminous IRAS sample by Sanders et al. (1991). The SP sample has 38 galaxies including interaction class 4 of Solomon & Sage (1988), interaction class 3 & 4 of Sanders et al. (1991), and closely interacting pairs from Combes et al. (1994). The definitions of "weakly perturbed" and "strongly perturbed" are given in the references listed above, SP galaxies being those identified as the final stages of mergers. In addition, we have constructed a sample made of 58 member galaxies in Virgo cluster, including both bright (Kenney & Young 1988ab) and faint spirals (Boselli et al. 1995). In the SP and VC sample, 3 and 18 galaxies have only upper limits in CO, respectively.

In Fig. 2, we plot $\mathrm{M_{H_2}}$ against $\mathrm{L_B}$ for the VC, WP, and SP samples along with a solid line representing the power law derived from our isolated galaxies sample (Eq. 1). We have analyzed the residuals of each subsample with respect to the isolated galaxies template, and none of the three subsamples can be distinguished from the isolated galaxy template. In Table 1, we summarize the median values of the residuals and the semi-interquartile distances which measure the dispersion of the distribution. The deviation of the residuals from zero value are statistically negligible, and this fact indicates that neither the optical luminosity *nor the molecular gas content* as measured in CO are significantly affected by tidal interactions. This contradicts the previous reports of enhanced molecular gas content among strongly interacting pairs (Braine & Combes 1993, Combes et al 1994). Virgo spirals show a gas content similar to isolated galaxies as has been previously suggested (see Boselli 1994 and references therein).

The relation between $\mathrm{L_{FIR}}$ and $\mathrm{M_{H_2}}$ is plotted in Fig. 3 for the three subsamples along with the power law relation obtained from the isolated galaxy sample. While the Virgo spirals and WP sample galaxies follow the same $\mathrm{L_{FIR}}$-$\mathrm{M_{H_2}}$ relation as the isolated galaxy sample, the SP sample galaxies show a clear deviation – enhanced FIR emission for given molecular gas content, already known in the literature as increase "star formation efficiency" ($\mathrm{L}_{FIR}/\mathrm{M}_{H_2}$ ratio – e.g. Sanders et al. 1991). The FIR luminosity of the SP sample galaxies lies mostly within the range covered by the isolated galaxy sample, but it extends to higher FIR luminosity and has a higher mean FIR luminosity than the isolated sample, requiring some extrapolation of Eqs. 1 & 2. We note however that the ranges of $\mathrm{M_{H_2}}$ and $\mathrm{L_B}$ covered by the SP and isolated comparison sample are the same, clearly indicating that the FIR emission is enhanced among the SP sample galaxies. We have improved the understanding of $\mathrm{L}_{FIR}/\mathrm{M}_{H_2}$ ratio by proper accounting the strong non-linear luminosity dependence while previous studies of $\mathrm{L}_{FIR}/\mathrm{M}_{H_2}$ ratio were performed with a simple assumption of no luminosity dependence and despite claims of enhanced molecular gas content in some cases.

Since we have shown that H_2 content is independent of tidal disruption or environment, any deviations from the template will indicate changes in the FIR emission. In Table 2 we summarize the statistics and probability of association in L_{FIR}/M_{H_2} distribution for the VC, WP, and SP samples with respect to the isolated galaxy sample. A zero value for the probability indicates that the compared distributions are statistically different from the isolated galaxy sample. Also included in Table 2 are the median and the semi–interquartile distance of the $\log[L_{FIR}/M_{H_2}]$ for all the samples as obtained from the cumulative distribution functions. All performed statistical tests indicate large differences in the distribution of the SP galaxies with respect to the isolated galaxies, as it was already clearly shown in Fig. 3. The VC galaxies show a L_{FIR}–M_{H_2} distribution very similar to the isolated galaxies as indicated by the similarity of their median values and by high statistical likelihood.

An evident result is that the star formation efficiency in the SP sample is enhanced on average by a factor 3.5 with respect to the isolated galaxy sample, consistent with the results in the literature (Sanders et al. 1986, Solomon & Sage 1988,Young & Scoville 1991), even when various non-linear dependences are properly accounted (the probability of the SP sample having the same distribution as the isolated sample is zero). Our new analysis also removes any uncertainty regarding variations in M_{H_2} as function of interaction strength (thus affecting L_{FIR}/M_{H_2} ratio) since no such variation is found. The weakly interacting systems show some marginal excess in SFE (30%, well within one sigma). This can be understood since observational separation between weak and strong interactions is not always straightforward, and some contamination exists between the two samples.

3.2. Barred and unbarred galaxies

Out of 196 galaxies in our sample with morphological classification listed in NED, 117 are classified as barred (38 isolated, 28 WP, 13 SP, and 38 VC) and 79 as unbarred (30 isolated, 15 WP, 14 SP, and 20 VC). The same analysis is now performed for the barred versus unbarred galaxies in order to test the previous claims that enhance star forming activity is associated with barred spirals (e.g., Young 1992).

In Fig. 4a, we plot L_B against M_{H_2} for the barred and unbarred galaxies, and no clear difference is seen between them, indicating that the total molecular mass is independent of their barred morphology. In fact L_B distributions of barred and unbarred galaxies are found indistinguishable by different statistical tests applied, and the same conclusion is drawn for their M_{H_2} distributions also ($< log(L_B) >_{bar} = 10.231$, $< log(L_B) >_{unbar} = 10.110$; $< log[M_{H_2}] >_{bar} = 9.195$, $< log[M_{H_2}] >_{unbar} = 9.110$).

We have also explored for any differences in L_{FIR}–M_{H_2} distribution as shown in Fig. 4b. Again the data overlap, and the FIR emission of the barred and unbarred galaxies is found indistinguishable by the statistical tests performed ($< log(L_{FIR}) >_{bar} = 9.691$, $< log(L_{FIR}) >_{unbar} = 9.687$). Thus the star formation efficiency seems independent of the barred morphology, as shown in the histogram of the ratio L_{FIR}/M_{H_2} in Fig. 5. The median values that are respectively $[L_{FIR}/M_{H_2}]_{unbarred} = 0.69$ ($\sigma = 1.59$) and $[L_{FIR}/M_{H_2}]_{barred} = 0.76$ ($\sigma = 1.58$). Since bar morphology and starburst activity are sometimes associated with tidal interactions, this result may indicate that the lifetime of a stellar bar, if transient, is much longer than the time scale for starburst.

4. Conclusions

Through the study of a carefully selected sample of isolated spiral galaxies, we have clearly established that the two important global physical quantities for tracing star forming activities, L_{FIR} and M_{H_2}, have non-linear dependence on another commonly cited global quantity L_B. Furthermore we show that simple power law relations can effectively describe these non-linear relations for spiral galaxies spanning four orders of magnitude in FIR and M_{H_2} and nearly three orders of magnitude in L_B. These non-linear relations are critically important in comparing different samples of galaxies since a simple normalization and the resulting residual dependence imply that samples consisting of the more luminous galaxies would show intrinsically larger ratios. Using the non-linear template relations obtained from the isolated galaxy sample, we have re-analyzed previous claims of enhanced molecular gas content and star formation through tidal interactions. We have also examined the effect of cluster environment and presence of stellar bars on the H_2 content and any enhancement of star formation.

In the frame defined by the optical luminosity, molecular gas content, and far infrared luminosity, we found that gravitational interaction affects only the FIR emission. We found no evidence for enhanced molecular gas content among the interacting galaxies, and we conclude that the previous such claims are due to the use of size normalization using L_B without properly accounting of the non-linear dependence. We do confirm that enhanced FIR emission (star formation) by tidal interaction is real. We found no evidence for enhanced star formation among barred galaxies in comparison with the unbarred galaxies.

The authors thank N. Scoville, P. Solomon and J. Sulentic for useful discussions. JP, AO and LV-M are partially supported by DGICYT (Spain) Grant PB93-0159 and Junta de Andalucía (Spain). MSY is supported by the NRAO Jansky Research Fellowship.

REFERENCES

Arimoto, N., Sofue, Y., & Tsujimoto T., 1996 PASJ, 48, 275

Buat, V., & Xu, C. 1996, A&A, 306, 61

Boselli, A. 1994, A&A, 292, 1

Boselli, A., Casoli, F., & Lequeux, J. 1995, A&A, 110, 52

Braine, J., & Combes, F. 1993, A&A, 269, 7

Burstein, D., & Heiles, C. 1984, ApJS, 54, 33

Cohen, R. A., Dame, T. M., Garay, G., Montani, J., Rubio, M., & Thaddeus, P. 1988, ApJ, 331, L95

Combes, F., Prugniel, P., Rampazzo, R., & Sulentic, J. W. 1994, A&A, 281, 725

de Vaucouleurs, G., de Vaucouleurs, A., Corwin, H. G., Buta, R. J., Paturel & G., & Fouqué, P. 1991, Third Reference Catalogue of Bright Galaxies. (New York: Springer–Verlag) (RC3)

Devereux, N. A., & Hameed, S. 1997, AJ, 113, 599

Feigelson, E. D., & Nelson, P. I. 1985, ApJ, 293, 192

Helou, G., Khan, I.R., Malek, L., & Boehmer, L. 1988, ApJS, 68, 151.

Isobe, T., & Feigelson, E. D. 1990, BAAS, 22, 917

Isobe, T., Feigelson, E. D., & Nelson, P. I. 1986, ApJ, 306, 490

Kenney, J. D., & Young, J. S. 1988a, ApJS, 66, 261

Kenney, J. D., & Young, J. S. 1988b, ApJ, 326, 588

LaValley, M., Isobe, T. & Feigelson, E.D. "ASURV", 1992, BAAS, in The new software report for ASURV Rev. 1.1.

Maloney, P., & Wolfire, M. 1997, in CO: Twenty-Five Years of Millimeter-Wave Spectroscopy, eds. W. B. Latter et al., (Dordrecht: Kluwer), p.299

Roberts, M. S., & Haynes, M. P. 1994, ARA&A, 32, 115

Rubio, M., Garay, G., Montani, J., & Thaddeus, P. 1991, ApJ, 368, 173

Sage, L. J. 1993, A&A, 272, 123

Sage, L. J., & Solomon, P. M. 1989, ApJ, 342, L15

Sakamoto, S. 1996, ApJ, 462, 215

Sanders, D. B., Scoville, N. Z., & Soifer, B. T. 1991, ApJ, 370, 158

Sanders, D. B., Scoville, N. Z., Young, J. S., Soifer, B. T., Schloerb, F. P., Rice, W. L., Danielson, G. E. 1986, ApJ, 305, L45

Savage, B. D., & Mathis J. S. 1979, ARA&A, 17, 73

Sofue, Y. Wakamatsu, K., Taniguchi, Y., & Nakai, N. 1993, PASJ 45, 43

Solomon, P. M., Downes, D., Radford, S. J. E., & Barrett, J. W. 1997, ApJ, 478, 144

Solomon, P. M., & Sage, L. J. 1988, ApJ, 334, 613

Tully, R. B. 1988, in Nearby Galaxies Catalog, (Cambridge: Cambridge Univ. Press)

Witt, A. N., Thronson, Jr., H. A., & Capuano, Jr., J. M. 1992, ApJ, 393, 611

Witt, A. N., & Gordon, K. D. 1996, ApJ, 463, 681

Wolfire, M.G., Hollenbach, D., & Tielens, A.G.G.M. 1993, ApJ, 402, 195.

Young, J. S. 1987, in Star Forming Regions, p. 557, ed. M. Peimbert & J. Jugaku

Young, J. S., Allen, L., Kenney, J. D. P., Lesser, A., & Rownd, B. 1996, AJ, 1996, 1903

Young, J. S., & Scoville, N. Z. 1991, ARA&A, 29, 581

Young, J. S. 1992, in The Environment and Evolution of Galaxies, eds. J. M. Shull & H. A. Thronson, Jr. (Kluwer Academic Publishers: Dordrecht), p. 295

Young, J. S., Xie, S., Kenney, J. D. P., & Rice, W. L. 1989, ApJSS, 70, 699

This 2-column preprint was prepared with the AAS LaTeX macros v4.0.

Fig. 1.— The dependence of L_B and L_{FIR} on M_{H_2} for the isolated galaxy sample. The solid lines correspond to the fitted power law given in Eq. 1.

Fig. 2.— The dependence of L_B on M_{H_2} for the three samples of interacting galaxies. The plotted line corresponds to the template power law derived from the isolated galaxies.

Fig. 3.— The dependence of L_{FIR} on M_{H_2} for the interacting galaxy sample.

Fig. 4.— The dependence of L_B and L_{FIR} on M_{H_2} for all galaxies in our sample, separated by barred and unbarred morphology.

Fig. 5.— Histogram of the star formation efficiency measured by the ratio $[L_{FIR}/M_{H_2}]$ for our full sample, divided into barred and unbarred galaxies.

Sample	Median	Q[a]
Isolated	0.043	0.17
W. Per.	0.204	0.21
S. Per.	0.101	0.27
Virgo	0.197	0.14

Table 1: Statistical parameters of the residuals relative to the M_{H_2}–L_B template obtained from isolated galaxies.

[a] Semi-interquartile distance. For a normal distribution $\sigma = 3/2$ Q.

	Isolated	Virgo	WP	SP
logrank statistic	—	1.103	2.193	5.769
Probability	—	0.270	0.028	0.000
Peto–Prentice	—	0.191	1.889	6.457
Probability	—	0.848	0.059	0.000
Median	0.633	0.583	0.737	1.171
Semi-interquartile	0.287	0.404	0.279	0.184

Table 2: Statistical parameters of $\log[L_{FIR}/M_{H_2}]$ distribution for the studied samples as compared with the isolated galaxies template (from Astronomy Survival Analysis package).

Figure 1

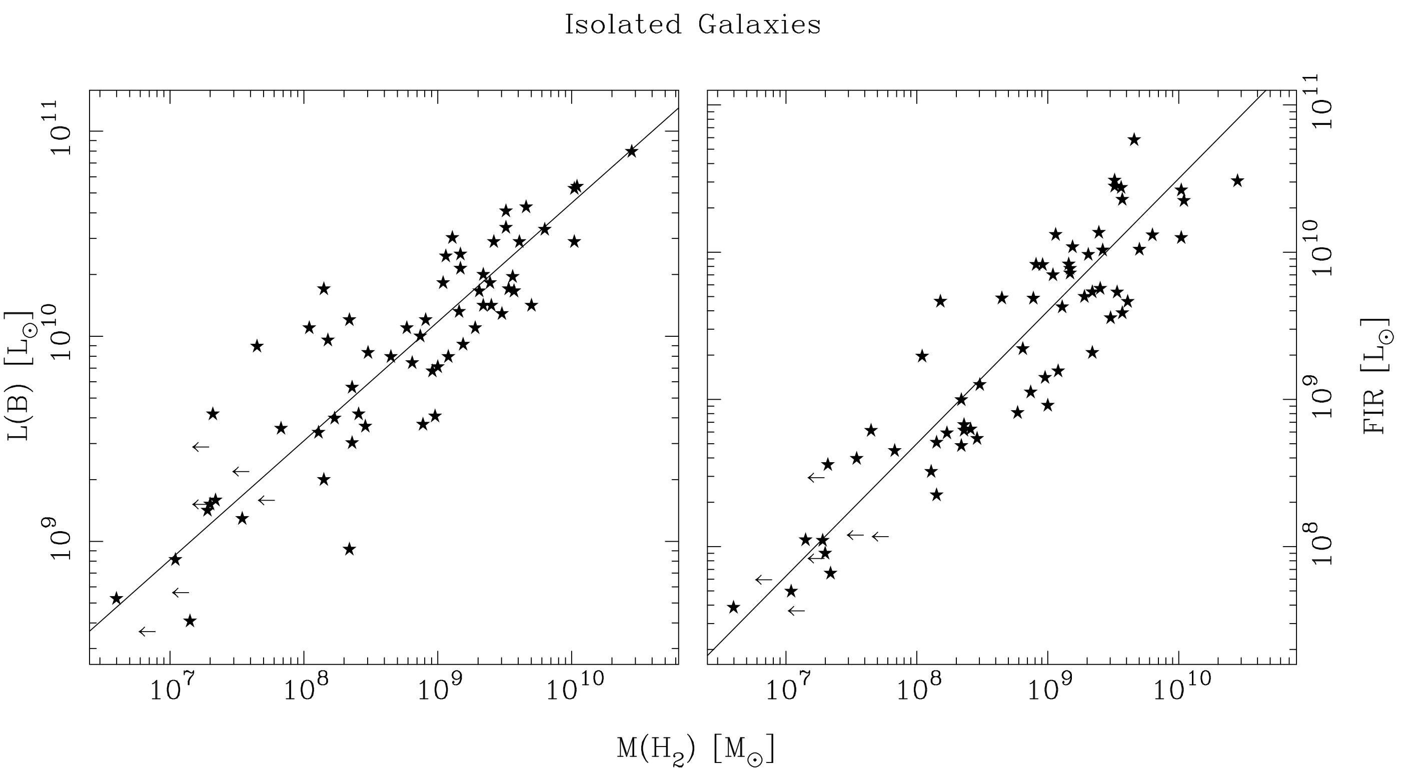

Figure 2

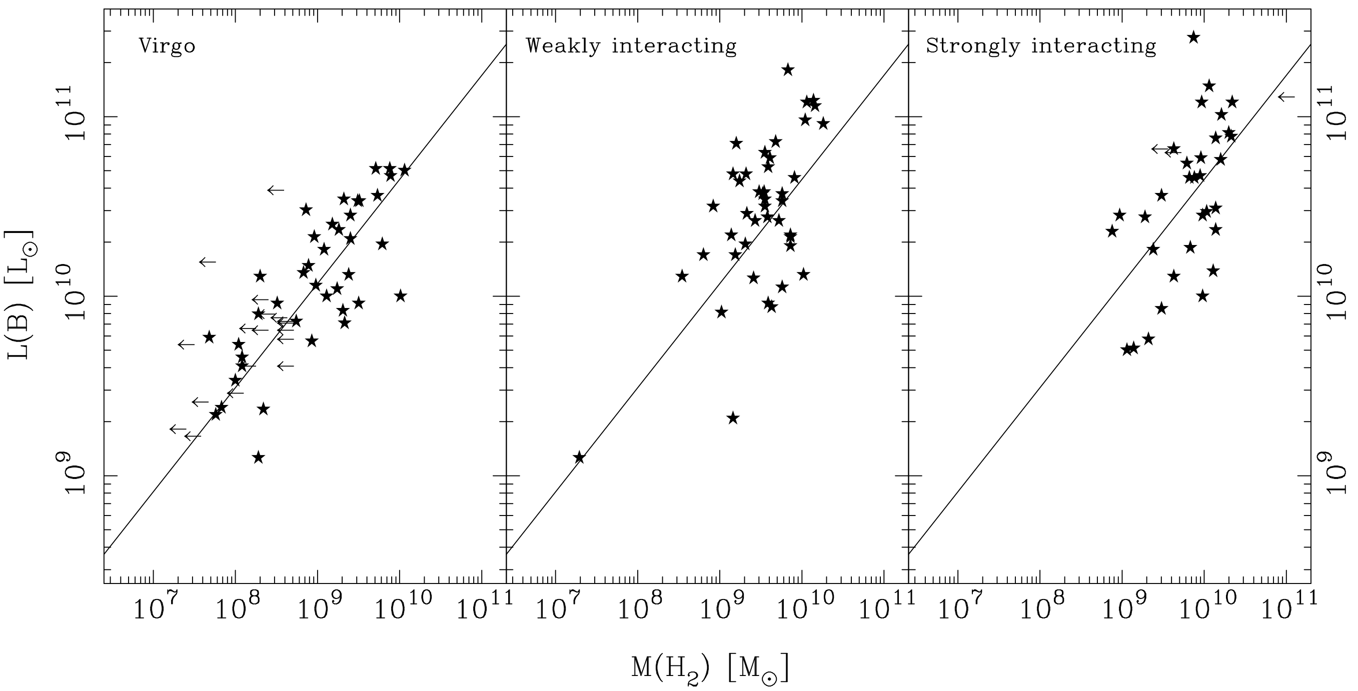

Figure 3

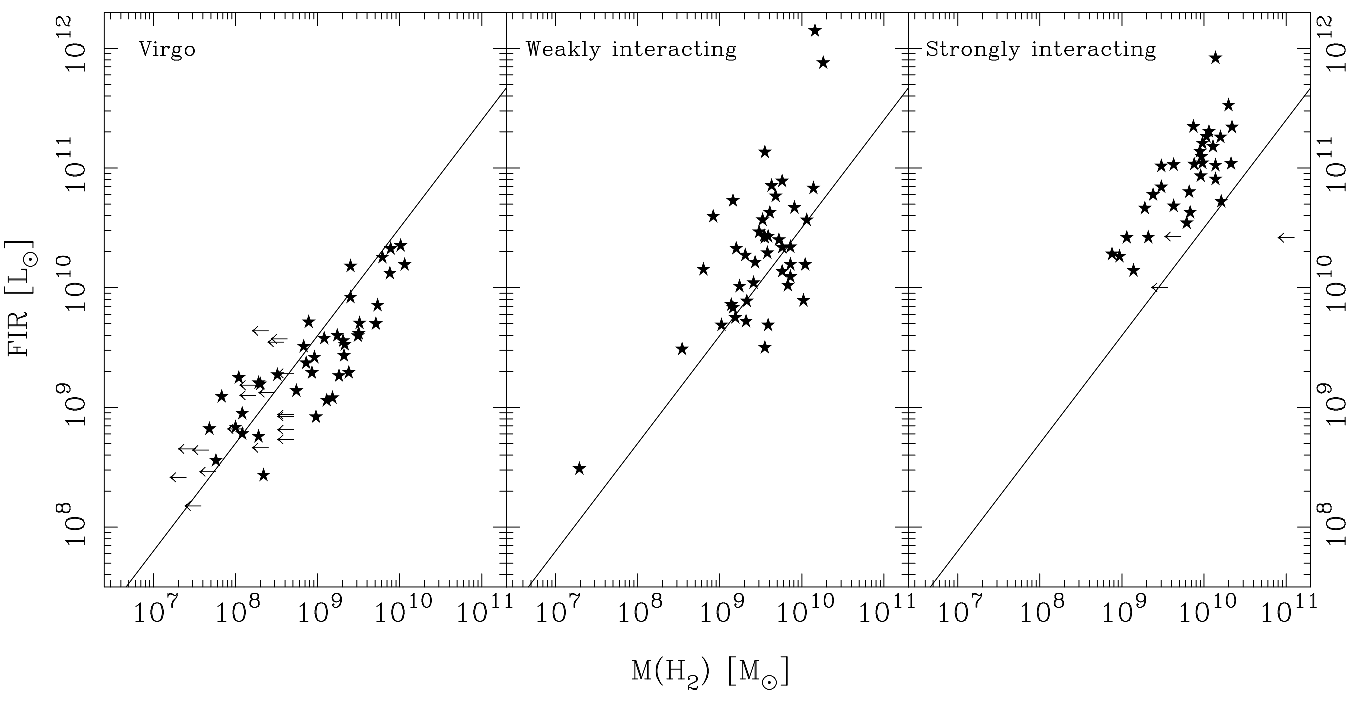

Figure 4

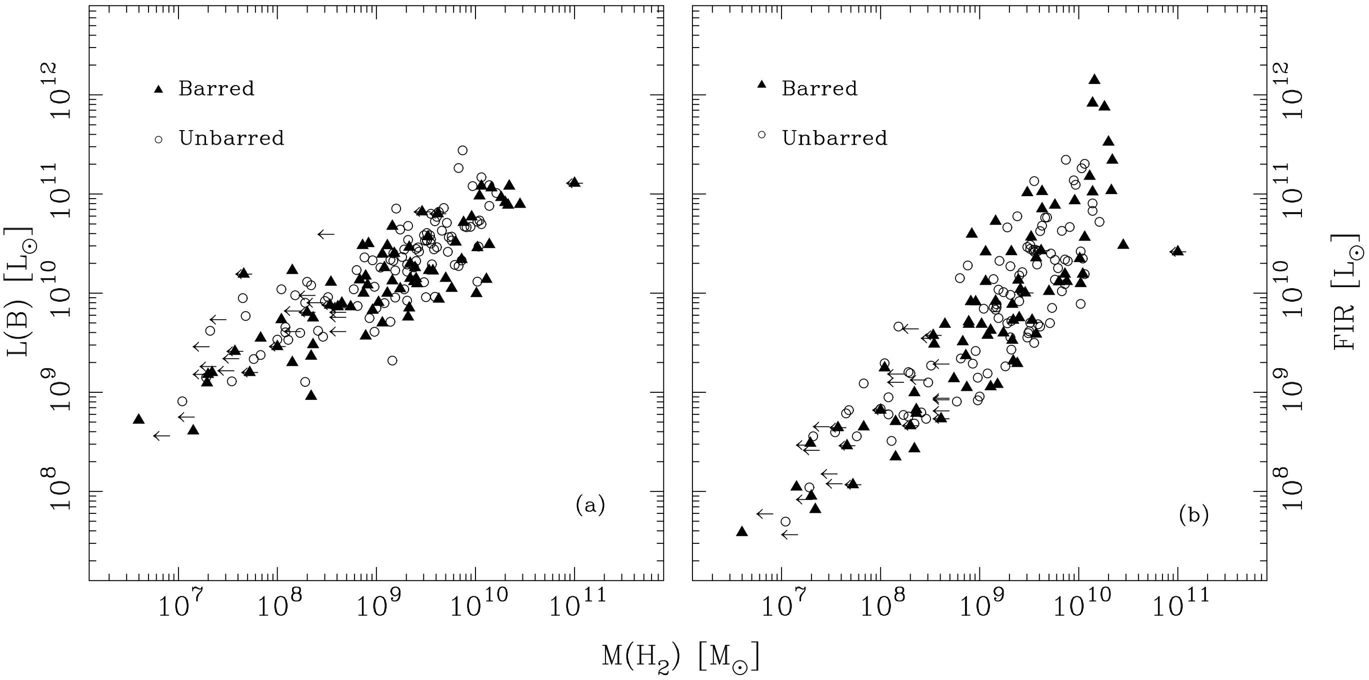

Figure 5